ON SURFACE MESHES INDUCED BY LEVEL SET FUNCTIONS

MAXIM A. OLSHANSKII*, ARNOLD REUSKEN†, AND XIANMIN XU†‡

Abstract. The zero level set of a piecewise-affine function with respect to a consistent tetrahedral subdivision of a domain in $\mathbb{R}^3$ is a piecewise-planar hyper-surface. We prove that if a family of consistent tetrahedral subdivions satisfies the *minimum angle condition*, then after a simple post-processing this zero level set becomes a consistent surface triangulation which satisfies the *maximum angle condition*. We treat an application of this result to the numerical solution of PDEs posed on surfaces. We show that the nodal basis of a P_1 finite element space with respect to this surface triangulation is L^2-stable, provided a natural scaling is used. Furthermore, the issue of stability of the nodal basis with respect to the H^1-norm is addressed.

Key words. surface finite elements, level set function, surface triangulation, maximum angle condition

1. Introduction. Surface triangulations occur in, for example, visualization, shape optimization, surface restoration and in applications where differential equations posed on surfaces are treated numerically. Hence, properties of surface triangulations such as shape regularity and angle conditions are of interest. For example, angle conditions are closely related to approximation properties and stability of corresponding finite element [1, 2].

In this note, we are interested in the properties of a surface triangulation if one considers the zero level of a piecewise-affine function with respect to a consistent tetrahedral subdivision of a domain in $\mathbb{R}^3$. The zero level of a piecewise-affine function is a piecewise-planar hyper-surface consisting of triangles and quadrilaterals. Each quadrilateral can be divided into two triangles in such a way that the resulting surface triangulation satisfies the following property proved in this paper: if the volume tetrahedral subdivision satisfies a minimum angle condition, then the corresponding surface triangulation satisfies a maximum angle condition. We show that the maximum angle occuring in the surface triangulation can be bounded by a constant $\phi_{\max} < \pi$ that depends only on a stability constant for the family of tetrahedral subdivisions.

The paper also discusses a few implications of this property for the numerical solution of surface partial differential equations. Numerical methods for surface PDEs are studied in e.g., [5, 4, 8, 3, 6, 11]. We derive optimal approximation properties of P_1 finite element functions with respect to the surface triangulation and a uniform bound for the condition number of the scaled mass matrix. We also show that the condition number of the (scaled) stiffness matrix can be very large and is sensitive to the distribution of the vertices of tetrahedra close to the surface. Some numerical examples illustrate the analysis of the paper.

2. Surface meshes induced by regular bulk triangulations. Consider a smooth surface Γ in three dimensional space. For simplicity, we assume that Γ is connected and has no boundary. Let $\Omega \subset \mathbb{R}^3$ be a bulk domain which contains Γ. Let $\{\mathcal{T}_h\}_{h>0}$ be a family of tetrahedral triangulations of the domain Ω. These

*Department of Mathematics, University of Houston, Houston, Texas 77204-3008 and Dept. Mechanics and Mathematics, Moscow State University, Moscow 119899 (molshan@math.uh.edu).

†Institut für Geometrie und Praktische Mathematik, RWTH-Aachen University, D-52056 Aachen, Germany (reusken@igpm.rwth-aachen.de,xu@igpm.rwth-aachen.de).

‡LSEC, Institute of Computational Mathematics and Scientific/Engineering Computing, NCMIS, AMSS, Chinese Academy of Sciences, Beijing 100190, China (xmxu@lsec.cc.ac.cn).

triangulations are assumed to be regular, consistent and stable. To simplify the presentation we assume that this family of triangulations is *quasi-uniform*. The latter assumption, however, is not essential for our analysis.

We assume that for each $\mathcal{T}_h$ a polygonal approximation of Γ, denoted by Γ_h, is given with the following properties. Γ_h is a $C^{0,1}$ surface without boundary and Γ_h can be partitioned in planar triangular segments. We assume that Γ_h is *consistent with the outer triangulation* $\mathcal{T}_h$ in the following sense. For any tetrahedron $S_T \in \mathcal{T}_h$ such that $\mathrm{meas}_2(S_T \cap \Gamma_h) > 0$ define $T = S_T \cap \Gamma_h$. We assume that every $T \in \Gamma_h$ is a *planar* segment and thus it is either a triangle or a quadrilateral. Each quadrilateral segment can be divided into two triangles, so we may assume that every T is a triangle.

Let $\mathcal{F}_h$ be the set of all triangular segments T, then Γ_h can be decomposed as

$$\Gamma_h = \bigcup_{T \in \mathcal{F}_h} T. \tag{2.1}$$

The most prominent example of such a surface triangulation is obtained in the context of level set techniques. Assume that Γ is represented as the zero level of a level set function ϕ and that ϕ_h is a continuous linear finite element approximation on the outer tetrahedral triangulation $\mathcal{T}_h$. Then if we define Γ_h to be the zero level of ϕ_h then Γ_h consists of piecewise planar segments and is consistent with $\mathcal{T}_h$. As an example, consider a sphere Γ, represented as the zero level of its signed distance function. For ϕ_h we take the piecewise linear nodal interpolation of this distance function on a uniform tetrahedral triangulation $\mathcal{T}_h$ of a domain that contains Γ. The zero level of this interpolant defines Γ_h and is illustrated in Fig. 2.1.

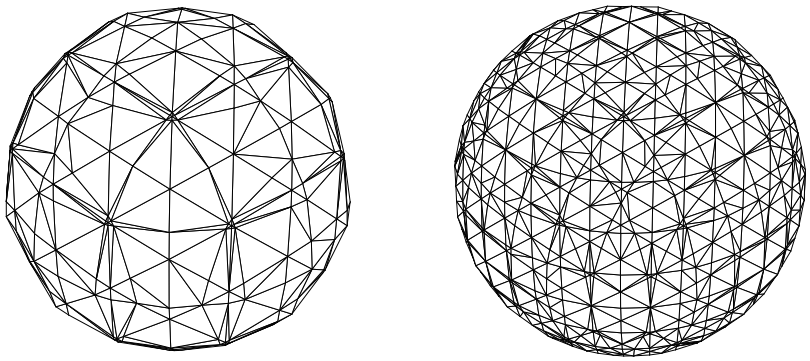

FIG. 2.1. *Approximate interface Γ_h for an example of a sphere, resulting from a coarse tetrahedral triangulation (left) and after one refinement (right).*

In the setting of level set methods, such surface triangulations induced by a finite element level set function on a regular outer tetrahedral triangulation are very natural and easy to construct. A surface triangulation Γ_h that is consistent with the outer triangulation may be the result of another method than the level set method. In the remainder we only need that Γ_h is consistent to the outer triangulation and not that it is generated by a level set technique.

Note that the triangulation $\mathcal{F}_h$ is *not* necessarily regular, i.e. elements from T may have *very small inner angles* and the *size of neighboring triangles can vary strongly*, cf. Fig. 2.1. In the next section we prove that, provided each quadrilateral is divided into two triangles properly, the induced surface triangulation is such that the *maximal angle condition* [1] is satisfied.

3. The maximal angle condition. The surface triangulation $\Gamma_h = \cup_{T\in\mathcal{F}_h} T$ is assumed to be consistent with the outer tetrahedral triangulation $\mathcal{T}_h$, as defined in section 2. The family of outer tetrahedral triangulations $\{\mathcal{T}_h\}_{h>0}$ is assumed to be regular, i.e., it contains no hanging nodes and the following stability property holds:

$$\sup_{h>0}\sup_{S\in\mathcal{T}_h} \rho(S)/r(S) \;\leq\; \alpha < \infty, \tag{3.1}$$

where $\rho(S)$ and $r(S)$ are the diameters of the smallest ball that contains S and the largest ball contained in S, respectively. Although the surface mesh Γ_h induced by $\mathcal{T}_h$ can be highly shape irregular, the following lemma shows that a *maximum angle* property holds.

LEMMA 3.1. *Assume an outer triangulation $\mathcal{T}_h$ from the regular family $\{\mathcal{T}_h\}_{h>0}$ and let Γ_h be consistent with $\mathcal{T}_h$. For any $S \in \mathcal{T}_h$ there exists $\phi_{\min} > 0$, depending only on α from* (3.1)*, such that:*

a) if $T = S \cap \Gamma_h$ is a triangle element, then

$$0 < \phi_{i,T} \leq \pi - \phi_{\min} \quad i = 1, 2, 3, \tag{3.2}$$

holds, where $\phi_{i,T}$ are the inner angles of the element T.

b) if $T = S \cap \Gamma_h$ is a quadrilateral element, then

$$\phi_{i,T} \geq \phi_{\min}, \quad i = 1, 2, 3, 4, \tag{3.3}$$

holds, where $\phi_{i,T}$ are the inner angles of the element T.

Proof. Take $S \in \mathcal{T}_h$. Let $\theta_{\min} > 0$ be such that all inner angles of all sides of S and all angles between edges of S and their opposite side are in the interval $[\theta_{\min}, \pi-\theta_{\min}]$. From the stability property it follows that

$$\frac{\pi}{2} > \theta_{\min} \geq c(\alpha) > 0$$

holds with a constant $c(\alpha)$ that depends only on α from (3.1).

We first treat the case where $T = S \cap \Gamma_h$ is a triangle $T = BCD$, as illustrated in Fig. 3.1. Consider the angle $\phi := \angle BCD$. Then either $\phi \leq \pi - \theta_{\min}$ and (3.2) is

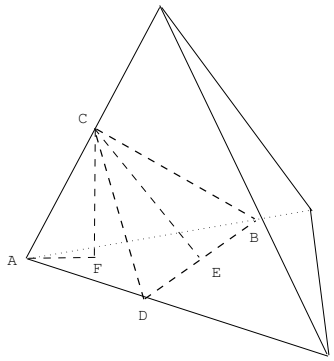

FIG. 3.1.

proved with $\phi_{\min} = \theta_{\min}$ or $\phi \in (\pi - \theta_{\min}, \pi)$. Hence, we treat the latter case. Note that

$$\frac{|CF|}{|AC|} = \sin(\angle CAF) \geq \sin\theta_{\min}$$

and $\angle BDC < \pi - \phi < \theta_{\min} < \frac{\pi}{2}$. Take E on the line through DB such that $CE \perp DB$, and F in the plane through ABD such that CF is perpendicular to this plane. Hence, $|CF| \leq |CE|$ holds. Using the sine rule we get

$$\begin{aligned}\sin(\angle ADC) &= \frac{|AC|}{|CD|}\sin(\angle CAD) \leq \frac{|AC|}{|CD|} \leq \frac{1}{\sin\theta_{\min}}\frac{|CF|}{|CD|} \leq \frac{1}{\sin\theta_{\min}}\frac{|CE|}{|CD|} \\ &= \frac{1}{\sin\theta_{\min}}\sin(\angle BDC) \leq \frac{\sin(\pi-\phi)}{\sin\theta_{\min}} = \frac{\sin(\phi)}{\sin\theta_{\min}} < 1.\end{aligned}$$

Hence, $\angle ADC \leq \arcsin(\frac{\sin\phi}{\sin\theta_{\min}}) \leq 2\frac{\sin\phi}{\sin\theta_{\min}}$ holds. This yields

$$\angle ADB < \angle ADC + \angle CDB \leq 2\frac{\sin\phi}{\sin\theta_{\min}} + \pi - \phi.$$

With the same arguments we obtain

$$\angle ABD \leq 2\frac{\sin\phi}{\sin\theta_{\min}} + \pi - \phi.$$

Since $\angle DAB \leq \pi - \theta_{\min}$ and $\angle DAB = \pi - (\angle ADB + \angle ABD)$ we get

$$\theta_{\min} \leq 4\frac{\sin\phi}{\sin\theta_{\min}} + 2\pi - 2\phi. \tag{3.4}$$

For $\phi \in (\pi - \theta_{\min}, \pi)$ the inequality (3.4) holds iff $\phi \leq \phi_0$, where ϕ_0 is the unique solution in $(\frac{1}{2}\pi, \pi)$ of $2\sin\phi_0 + (\pi - \phi_0)\sin\theta_{\min} = \frac{1}{2}\theta_{\min}\sin\theta_{\min}$. This proves the result in a).

We now consider the case where $T = S \cap \Gamma_h$ is a quadrilateral $T = ABCD$, as illustrated in Fig. 3.2. Consider the angle $\phi := \angle DAB$. Then either $\phi \in (0, \theta_{\min})$ or

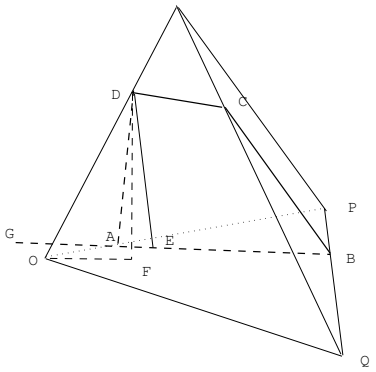

FIG. 3.2.

$\phi \in [\theta_{\min}, \pi)$. We only should treat the former case. Take E on the line through AB such that $DE \perp AB$, and F in the plane through OPQ such that DF is perpendicular to this plane. Hence, $|DF| \leq |DE|$ holds and

$$\sin\phi = \frac{|DE|}{|AD|}.$$

Furthermore, using $\frac{|DF|}{|OD|} = \sin(\angle DOF) \geq \sin\theta_{\min}$ we get

$$\sin(\angle OAD) = \frac{|OD|}{|AD|}\sin(\angle AOD) \leq \frac{|OD|}{|AD|} \leq \frac{1}{\sin\theta_{\min}}\frac{|DF|}{|AD|}$$
$$\leq \frac{1}{\sin\theta_{\min}}\frac{|DE|}{|AD|} = \frac{\sin\phi}{\sin\theta_{\min}} < 1.$$

This implies

$$\angle OAD \leq \arcsin\big(\frac{\sin\phi}{\sin\theta_{\min}}\big) \leq 2\frac{\sin\phi}{\sin\theta_{\min}}.$$

Hence, since $\angle DAB = \phi \leq 2\sin\phi$, we obtain

$$\angle OAB < \angle OAD + \angle DAB \leq \big(1 + \frac{1}{\sin\theta_{\min}}\big)2\sin\phi.$$

Using $\angle OAB = \pi - \angle PAB$ and $\angle PAB < \pi - \angle OPQ < \pi - \theta_{\min}$ results in

$$\theta_{\min} < \big(1 + \frac{1}{\sin\theta_{\min}}\big)2\sin\phi. \tag{3.5}$$

For $\phi \in (0, \theta_{\min})$ the inequality (3.5) holds iff $\phi \geq \phi_0$, where ϕ_0 is the unique solution in $(0, \frac{1}{2}\pi)$ of $\theta_{\min} = \big(1 + \frac{1}{\sin\theta_{\min}}\big)2\sin\phi_0$. Thus the result in b) holds.
□

The lemma readily yields the following result.

THEOREM 3.2. *Consider a regular family of tetrahedral triangulations $\{\mathcal{T}_h\}_{h>0}$ and a surface triangulation $\Gamma_h = \cup_{T\in\mathcal{F}_h} T$ that is consistent to $\mathcal{T}_h$. Assume that any quadrilateral element $T = S \cap \Gamma_h$, $S \in \mathcal{T}_h$, is divided in two triangles by connecting its vertex with largest inner angle with its opposite vertex. The resulting surface triangulation satisfies the following maximal angle condition. There exists $\phi_{\min} > 0$ depending only on α from* (3.1) *such that:*

$$0 < \sup_{T\in\mathcal{F}_h} \phi_{i,T} \leq \pi - \phi_{\min} \quad i = 1, 2, 3, \tag{3.6}$$

where $\phi_{i,T}$ are the inner angles of the element T.

Proof. If $T = S \cap \Gamma_h$ is a triangle, then (3.6) directly follows from (3.2). Let $T = S \cap \Gamma_h$ be a quadrilateral, with its four inner angles denoted by $\theta_4 \geq \theta_3 \geq \theta_2 \geq \theta_1 > 0$. From the result in (3.3) we have $\theta_i \geq \phi_{\min}$ for all i. The vertex with angle θ_4 is connected with the opposite vertex. Let T_1 be one of the resulting triangles. One of the angles of T_1 is θ_j with $j \in \{1, 2, 3\}$. From $\theta_j \geq \phi_{\min}$ it follows that the other two angles are both bounded by $\pi - \phi_{\min}$. Furthermore, from $\theta_j = 2\pi - \theta_4 - \sum_{i=1, i\neq j}^{3} \theta_i \leq 2\pi - \theta_j - 2\phi_{\min}$ it follows that $\theta_j \leq \pi - \phi_{\min}$ holds. □

In the remainder we assume that quadrilaterals are subdivided in the way as explained in Theorem 3.2. Hence, the inner angles in the surface triangulation $\mathcal{F}_h$ are bounded by a constant $\theta^* < \pi$ that depends only on the stability (close to Γ) of the outer tetrahedral triangulation $\mathcal{T}_h$. In particular θ^* is *independent of h and of how Γ_h intersects the outer triangulation $\mathcal{T}_h$.*

4. Application in a finite element method. In this section, we use the maximum angle property of the surface triangulation to derive an optimal finite element interpolation result. On $\mathcal{F}_h$ we consider the space of linear finite element functions:

$$V_h = \{v_h \in \mathcal{C}(\Gamma_h) : v_h \in \mathcal{P}_1(T) \quad \text{for all} \quad T \in \mathcal{F}_h\}. \tag{4.1}$$

This finite element space is the same as the one studied by Dziuk in [5], but an important difference is that in the approach in [5] the triangulations have to be shape regular. In general, the finite element space V_h is different from the surface finite element space constructed in [9, 8].

Below we derive an approximation result for the finite element space V_h. Since the discrete surface Γ_h varies with h, we have to explain in which sense Γ_h is close to Γ. For this we use a standard setting applied in the analysis of discretization methods for partial differential equations on surfaces, e.g. [5, 4, 6, 7, 9].

Let $U := \{ x \in \mathbb{R}^3 \mid \operatorname{dist}(x,\Gamma) < c \}$ be a sufficiently small neighborhood of Γ. We define $\mathcal{T}_h^\Gamma := \{ T \in \mathcal{T}_h \mid \operatorname{meas}_2(T \cap \Gamma_h) > 0 \}$, i.e., the collection of tetrahedra which intersect the discrete surface Γ_h, and assume that $\mathcal{T}_h^\Gamma \subset U$. Let d be the signed distance function to Γ, with $d < 0$ in the interior of Γ,

$$d : U \to \mathbb{R}, \qquad |d(x)| := \operatorname{dist}(x,\Gamma) \quad \text{for all } x \in U.$$

Thus Γ is the zero level set of d. Note that $\mathbf{n}_\Gamma = \nabla d$ on Γ. We define $\mathbf{n}(x) := \nabla d(x)$ for $x \in U$. Thus $\mathbf{n}$ is the outward pointing normal on Γ and $\|\mathbf{n}(x)\| = 1$ for all $x \in U$. Here and in the remainder $\|\cdot\|$ denotes the Euclidean norm on $\mathbb{R}^3$. We introduce a local orthogonal coordinate system by using the projection $\mathbf{p} : U \to \Gamma$:

$$\mathbf{p}(x) = x - d(x)\mathbf{n}(x) \quad \text{for all } x \in U.$$

We assume that the decomposition $x = \mathbf{p}(x) + d(x)\mathbf{n}(x)$ is unique for all $x \in U$. Note that $\mathbf{n}(x) = \mathbf{n}\big(\mathbf{p}(x)\big)$ for all $x \in U$. For a function v on Γ, its extension is defined as

$$v^e(x) := v(\mathbf{p}(x)), \quad \text{for all } x \in U. \tag{4.2}$$

The outward pointing (piecewise constant) unit normal on Γ_h is denoted by $\mathbf{n}_h$. Using this local coordinate system we introduce the following assumptions on Γ_h:

$$\mathbf{p} : \Gamma_h \to \Gamma \quad \text{is bijective,} \tag{4.3}$$

$$\max_{x \in \Gamma_h} |d(x)| \lesssim h^2, \tag{4.4}$$

$$\max_{x \in \Gamma_h} \|\mathbf{n}(x) - \mathbf{n}_h(x)\| \lesssim h. \tag{4.5}$$

In (4.4)-(4.5) we use the common notation, that the inequality holds with a constant independent of h. In (4.5), only $x \in \Gamma_h$ are considered for which $\mathbf{n}_h(x)$ is well-defined. Using these assumptions, the following result is derived in [5].

LEMMA 4.1. *For any function $u \in H^2(\Gamma)$, we have, for arbitrary $T \in \mathcal{F}_h$ and $\tilde{T} := \mathbf{p}(T)$:*

$$\|u^e\|_{0,T} \sim \|u\|_{0,\tilde{T}}, \tag{4.6}$$

$$|u^e|_{1,T} \sim |u|_{1,\tilde{T}}, \tag{4.7}$$

$$|u^e|_{2,T} \lesssim |u|_{2,\tilde{T}} + h|u|_{1,\tilde{T}}, \tag{4.8}$$

where $A \sim B$ means $B \lesssim A \lesssim B$ and the constants in the inequalities are independent of T and of h.

4.1. Finite element interpolation error. Based on the results in Lemma 4.1, the maximum angle property and the approximation results derived in [1] we easily

obtain an optimal bound for the interpolation error in the space V_h. Consider the standard finite element nodal interpolation $I_h : C(\Gamma_h) \to V_h$:

$$(I_h v)(x) = v(x), \quad \text{for all } \; x \in \mathcal{V}, \tag{4.9}$$

with $\mathcal{V}$ the set of vertices of the triangles in Γ_h.

THEOREM 4.2. *For any $u \in H^2(\Gamma)$ we have*

$$\|u^e - I_h u^e\|_{L^2(\Gamma_h)} \lesssim h^2 \|u\|_{H^2(\Gamma)}, \tag{4.10}$$
$$\|u^e - I_h u^e\|_{H^1(\Gamma_h)} \lesssim h \|u\|_{H^2(\Gamma)}. \tag{4.11}$$

Proof. From standard interpolation theory we have

$$\|u^e - I_h u^e\|_{L^2(T)} \lesssim h^2 |u^e|_{2,T},$$

where the constant in the upper bound is independent of (the shape of) T. Using the result in (4.8) and summing over $T \in \mathcal{F}$ proves the result (4.10). For the interpolation error bound in the H^1-norm we use the results from [1]. For the interpolation error bounds derived in that paper the maximum angle property is essential. From [1] we get

$$\|u^e - I_h u^e\|_{H^1(T)} \lesssim h \|u\|_{H^2(T)}.$$

Due to the maximum angle property the constant in the upper bound is independent of T. Using the results in Lemma 4.1 and summing over $T \in \mathcal{F}_h$ we obtain the result (4.11). ∎

If one considers an $H^1(\Gamma)$ elliptic partial differential equation on Γ, the error for its finite element discretization in the surface space V_h can be analyzed along the same lines as in [5]. Using the interpolation error bounds in Theorem 4.2 and bounding the geometric errors (due to approximation of Γ by Γ_h) with the use of the assumptions (4.3)-(4.5) then results in optimal order discretization error bounds.

4.2. Conditioning of mass and stiffness matrix. Clearly the (strong) shape irregularity of the surface triangulation will influence the conditioning of the mass and stiffness matrices. Let N be the number of vertices in the surface triangulation and $\{\phi_i\}_{i=1}^N$ the nodal basis of the finite element space V_h. The mass and stiffness matrices are given by

$$\mathbf{M} = (m_{ij})_{i,j=1}^N, \quad \text{with} \quad m_{ij} = \int_{\Gamma_h} \phi_i \phi_j \, ds, \tag{4.12}$$

$$\mathbf{A} = (a_{ij})_{i,j=1}^N, \quad \text{with} \quad a_{ij} = \int_{\Gamma_h} \nabla_{\Gamma_h} \phi_i \nabla_{\Gamma_h} \phi_j \, ds. \tag{4.13}$$

We also need their scaled versions. Let $\mathbf{D}_M$ and $\mathbf{D}_A$ be the diagonals of $\mathbf{M}$ and $\mathbf{A}$, respectively. The scaled matrices are denoted by

$$\mathbf{M}^s = \mathbf{D}_M^{-\frac{1}{2}} \mathbf{M} \mathbf{D}_M^{-\frac{1}{2}}, \quad \mathbf{A}^s = \mathbf{D}_A^{-\frac{1}{2}} \mathbf{A} \mathbf{D}_A^{-\frac{1}{2}}.$$

From a simple scaling argument it follows that the spectral condition number of $\mathbf{M}^s$ is bounded uniformly in h and in the shape (ir)regularity of the surface triangulation. For completeness we include a proof.

THEOREM 4.3. *The following holds:*

$$\frac{2}{\sqrt{2}+2} \leq \frac{\langle \mathbf{M}\mathbf{v},\mathbf{v}\rangle}{\langle \mathbf{D}_M\mathbf{v},\mathbf{v}\rangle} \leq 4 \quad \textit{for all} \;\; \mathbf{v}\in\mathbb{R}^N,\; \mathbf{v}\neq 0.$$

Proof. The set of all vertices in $\mathcal{F}_h$ is denoted by $\mathcal{V} = \{\, \xi_i \mid 1 \leq i \leq N \,\}$. Let $\mathbf{v}\in\mathbb{R}^N$ and $v_h \in V_h$ be related by $v_h = \sum_{i=1}^N v_i\phi_i$, i.e., $v_i = v_h(\xi_i)$. Consider a triangle $T\in\mathcal{F}_h$ and let its three vertices be denoted by ξ_1,ξ_2,ξ_3. Using quadrature we obtain

$$\begin{aligned}\int_T v_h(s)^2\,ds &= \frac{|T|}{3}\big(\frac{1}{4}(v_1+v_2)^2+\frac{1}{4}(v_2+v_3)^2+\frac{1}{4}(v_3+v_1)^2\big)\\ &= \frac{|T|}{6}\big(v_1^2+v_2^2+v_3^2+v_1v_2+v_2v_3+v_3v_1\big).\end{aligned}$$

Hence, $\int_T v_h(s)^2\,ds \leq \frac{|T|}{3}\sum_{i=1}^3 v_i^2$ holds. From a sign argument it follows that at least one of the three terms v_1v_2, v_2v_3 or v_3v_1 must be positive. Without loss of generality we can assume $v_1v_2\geq 0$. Using $|v_2v_3+v_3v_1| \leq \frac{1}{\sqrt{2}}\big(v_1^2+v_2^2+v_3^2\big)$ we get

$$\int_T v_h(s)^2\,ds \geq \frac{|T|}{6}\big(v_1^2+v_2^2+v_3^2-\frac{1}{\sqrt{2}}(v_1^2+v_2^2+v_3^2)\big) = \frac{|T|}{6(\sqrt{2}+2)}\big(v_1^2+v_2^2+v_3^2\big).$$

Note that $\langle \mathbf{M}\mathbf{v},\mathbf{v}\rangle = \int_{\Gamma_h} v_h(s)^2\,ds = \sum_{T\in\mathcal{F}_h}\int_T v_h(s)^2\,ds$, and thus we obtain, with $\mathcal{V}(T)$ the set of the three vertices of T,

$$\frac{2}{\sqrt{2}+2}\frac{1}{12}\sum_{T\in\mathcal{F}_h}|T|\sum_{\xi\in\mathcal{V}(T)} v_h(\xi)^2 \leq \langle \mathbf{M}\mathbf{v},\mathbf{v}\rangle \leq 4\frac{1}{12}\sum_{T\in\mathcal{F}_h}|T|\sum_{\xi\in\mathcal{V}(T)} v_h(\xi)^2. \tag{4.14}$$

We observe that

$$\frac{1}{12}\sum_{T\in\mathcal{F}_h}|T|\sum_{\xi\in\mathcal{V}(T)} v_h(\xi)^2 = \frac{1}{12}\sum_{i=1}^N |\mathrm{supp}(\phi_i)|v_i^2 \tag{4.15}$$

holds. From the definition of $\mathbf{D}_M$ it follows that

$$\begin{aligned}\langle \mathbf{D}_M\mathbf{v},\mathbf{v}\rangle &= \sum_{i=1}^N \int_{\Gamma_h}\phi_i^2\,ds\,v_i^2 = \sum_{i=1}^N v_i^2 \sum_{T\in\mathrm{supp}(\phi_i)}\int_T \phi_i^2\,ds\\ &= \sum_{i=1}^N v_i^2 \sum_{T\in\mathrm{supp}(\phi_i)}\frac{|T|}{12} = \frac{1}{12}\sum_{i=1}^N |\mathrm{supp}(\phi_i)|v_i^2.\end{aligned} \tag{4.16}$$

Combination of the results in (4.14), (4.15) and (4.16) completes the proof. ∎

The diagonally scaled stiffness matrix $\mathbf{A}^s$ has a one dimensional kernel due to the constant nodal mode. Thus, we consider the effective condition number $\mathrm{cond}(\mathbf{A}^s) = \lambda_{\max}(\mathbf{A}^s)/\lambda_2(\mathbf{A}^s)$, where λ_2 is the minimal nonzero eigenvalue. We shall argue below that the condition number of $\mathbf{A}^s$ can not be bounded in general by a constant dependent exclusively on $\mathcal{T}_h$, but not on Γ_h. Indeed, assume a smooth closed surface Γ, with $|\Gamma| = 1$, and a smooth function u defined on Γ, such that $\|\nabla_\Gamma u\|_{L^2(\Gamma)} = \|u\|_{H^2(\Gamma)} = 1$. Let Γ_h be the zero level of the piecewise linear Lagrange interpolant of the signed

distance function to Γ. Denote $u_h = I_h u^e$, as in Theorem 4.2, and $\mathbf{v} = (v_1, \ldots, v_N)^T$ is the corresponding vector of nodal values. From the result in (4.11) we obtain

$$\langle \mathbf{A}\mathbf{v}, \mathbf{v} \rangle = \|\nabla_{\Gamma_h} u_h\|_{L^2(\Gamma_h)} = 1 + O(h). \tag{4.17}$$

On the other hand, if there is a node ξ in the volume triangulation $\mathcal{T}_h$ such that $\mathrm{dist}(\xi, \Gamma_h) < \varepsilon \ll 1$, then there can appear a triangle in $\mathcal{F}_h$ with a minimal angle of $O(\varepsilon)$. This implies that there is a diagonal element in $\mathbf{A}$ of order $O(\varepsilon^{-1})$. Without lost of generality we may assume $A_{11} = O(\varepsilon^{-1})$ and $v_1 = 1$. Thus we get

$$\langle \mathbf{D}_A \mathbf{v}, \mathbf{v} \rangle \geq A_{11} v_1^2 = O(\varepsilon^{-1}). \tag{4.18}$$

Comparing (4.17) and (4.18) we conclude that $\mathrm{cond}(\mathbf{A}^s) \geq O(\varepsilon^{-1})$, with $\varepsilon \to 0$. Results of numerical experiments in the next section demonstrate that the blow up of $\mathrm{cond}(\mathbf{A}^s)$ can be seen in some cases.

One might also be interested in a more general dependence of the eigenvalues of $\mathbf{A}^s$ on the distribution of tetrahedral nodes in $\mathcal{T}_h$ in a neighborhood of Γ_h. To a certain extend this question is addressed in [8].

A strong growth of the condition number of the scaled stiffness matrix as in (4.17)-(4.18) does not necessarily lead to a severe slown down of iterative solvers. This is illustrated and discussed in section 5. One possibility to reduce the condition number deterioration sketched above is to 'glue' together nodes of $\mathcal{F}_h$ which have a distance less than ε from each other, with some sufficiently small ε. We did not investigate this idea further.

5. Numerical experiment. In this section we present a few results of numerical experiments which illustrate the interpolation estimates from Theorem 4.2 and the conditioning of mass and stiffness matrices. Assume the surface Γ, which is the unit sphere $\Gamma = \{ x \in \mathbb{R}^3 \mid \|x\| = 1 \}$, is embedded in the bulk domain $\Omega = [-2, 2]^3$. The signed distance function to Γ is denoted by d. We construct a hierarchy of uniform tetrahedral triangulations $\{\mathcal{T}_h\}$ for Ω, with $h \in \{1/2, 1/4, 1/8, 1/16, 1/32\}$. Let d_h be the piecewise nodal Lagrangian interpolant of d. The triangulated surface is given by

$$\Gamma_h = \bigcup_{T \in \mathcal{F}_h} T = \{ x \in \Omega \mid d_h(x) = 0 \}.$$

The corresponding finite element space V_h consists of all piecewise affine functions with respect to $\mathcal{F}_h$, as defined in (4.1). For $h \in \{1/2, 1/4, 1/8, 1/16, 1/32\}$, the resulting dimensions of V_h are $N = 164, 812, 3500, 14264, 57632$, respectively. In agreement with the 2D nature of Γ_h, we have $N \sim h^{-2}$.

To illustrate the result of Theorem 4.2, we present the interpolation errors $\|u^e - I_h u^e\|_{L^2(\Gamma_h)}$ and $|u^e - I_h u^e|_{1,\Gamma_h}$ for the smooth function

$$u(x) = \frac{1}{\pi} x_1 x_2 \arctan(2x_3)$$

defined on the unit sphere, with $x = (x_1, x_2, x_3)^T$. The dependence of the interpolation errors on the number of degrees of freedom N is shown in Figure 5.1 (left). We observe the optimal error reduction behavior, consistent with the estimates in (4.10), (4.11).

Further, for the same sequence of meshes we compute the spectral condition numbers of the mass matrix $\mathbf{M}$ and the diagonally scaled mass matrix $\mathbf{M}^s$. The

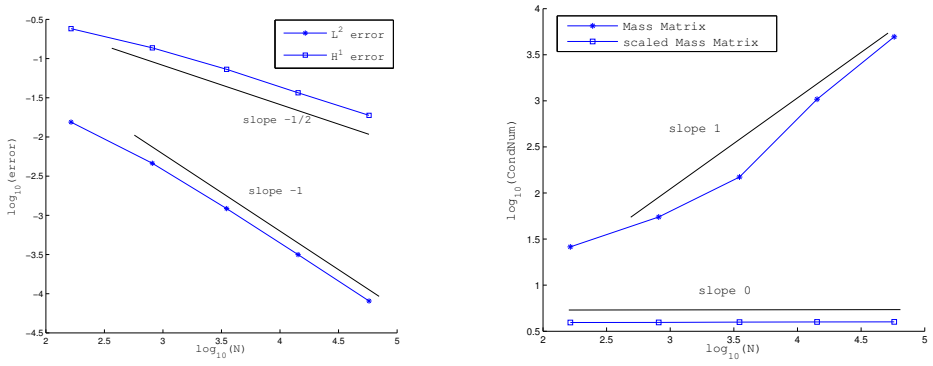

FIG. 5.1. *Left: Interpolation error as a function of # d.o.f.; Right: The condition number of the mass matrix as a function of of # d.o.f.*

dependence of the condition numbers on the number of degrees of freedom N is illustrated in Figure 5.1 (right). As was proved in Theorem 4.3, the scaled mass matrix has a uniformly bounded condition number.

We discussed in section 4.2 that the situation with the effective conditioning of the scaled stiffness matrix is more delicate. To illustrate numerically the dependence of $\mathrm{cond}(\mathbf{A}^s)$ on the position of Γ_h with respect to the outer triangulation, we perform the following series of experiments. Let Γ be the boundary of the unit sphere with the center located in $(0, 0, z_c)$. The discrete surface Γ_h is defined as described above, induced by the uniform outer triangulations. Now we compute the effective condition number of $\mathbf{A}^s$ varying both the mesh size of the outer grid h and the sphere's center location z_c. Results presented in Table 5.1 show the strong dependence of $\mathrm{cond}(\mathbf{A}^s)$ on the sphere location. The dramatic decrease of $\mathrm{cond}(\mathbf{A}^s)$ for $z_c = 0$ happens because in that case certain nodes of $\mathcal{T}_h$ lie exactly on Γ_h. Otherwise these nodes result in triangles in $\mathcal{F}_h$ that may have very sharp angles which then lead to the blow up of $\mathrm{cond}(\mathbf{A}^s)$. We also note that the interpolation errors (not shown) were (almost) independent on the position of Γ_h with respect to the outer triangulation.

In Table 5.1 we also show the total number of iterations for the diagonally preconditioned CG method applied to solve $\mathbf{Ax} = \mathbf{b}$ up to the relative residual tolerance of 10^{-10}. Note that the number of iterations depends on z_c in a much less dramatic way than $\mathrm{cond}(\mathbf{A}^s)$ does. The explanation of this observation is the following: Few nodes 'close' to Γ_h lead to a small number of outliers in the spectrum of $\mathbf{A}^s$. The small number of outliers in the spectrum is well known to result only in temporal stagnation period(s) in the convergence history of a Krylov subspace method rather than in a permanent low convergence rate, see, e.g., [10] and references cited therein. This phenomenon is illustrated in Figure 5.2, where we show the convergence histories of the CG method for $\mathbf{Ax} = \mathbf{b}$ with the diagonal preconditioner and different values of z_c.

Acknowledgments. This work has been supported in part by the DFG through grant RE1461/4-1 and the Russian Foundation for Basic Research through grants 12-01-91330, 12-01-00283.

REFERENCES

	$h = 1/4$		$h = 1/8$		$h = 1/16$	
z_c	cond($\mathbf{A}^s$)	N_{CG}	cond($\mathbf{A}^s$)	N_{CG}	cond($\mathbf{A}^s$)	N_{CG}
0.008	2.96e+04	178	2.15e+04	478	4.78e+04	1362
0.002	4.69e+05	187	3.30e+05	403	2.13e+05	1083
0.0005	7.49e+06	200	5.27e+06	429	3.35e+06	880
0.00025	3.00e+07	205	2.10e+07	440	1.34e+07	906
0.00005	7.49e+08	236	5.27e+08	497	3.34e+08	949
0.00001	3.66e+07	202	8.68e+07	514	3.95e+08	1020
0	4.62e+02	56	2.45e+03	142	1.10e+04	295

TABLE 5.1

Dependence of the effective condition number of $\mathbf{A}^s$ *and the number of CG steps* (N_{CG}) *on the position of* Γ_h

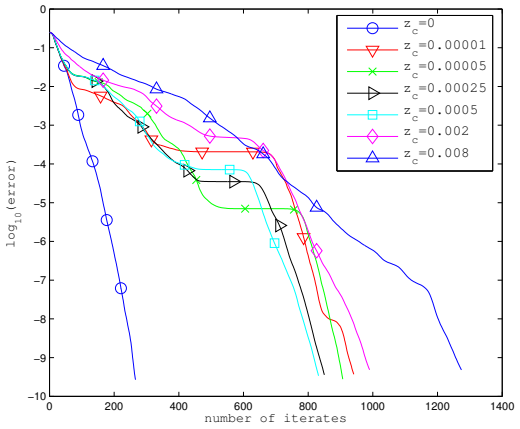

FIG. 5.2. *Convergence history of the diagonally preconditioned CG method for* $\mathbf{Ax} = \mathbf{b}$*, with* $h = 1/16$ *and different values of* z_c*.*

[1] I. Babuška and A. K. Aziz. On the angle condition in the finite element method. *SIAM J. Numer. Anal.*, 13:214–226, 1976.

[2] P. Ciarlet. *The Finite Element Method for Elliptic Problems*. North-Holland, Amsterdam, 1978.

[3] A. Demlow. Higher-order finite element methods and pointwise error estimates for elliptic problems on surfaces. *SIAM J. Numer. Anal.*, 47:805–827, 2009.

[4] A. Demlow and G. Dziuk. An adaptive finite element method for the Laplace-Beltrami operator on implicitly defined surfaces. *SIAM J. Numer. Anal.*, 45:421–442, 2007.

[5] G. Dziuk. Finite elements for the Beltrami operator on arbitrary surfaces. In S. Hildebrandt and R. Leis, editors, *Partial differential equations and calculus of variations*, volume 1357 of *Lecture Notes in Mathematics*, pages 142–155. Springer, 1988.

[6] G. Dziuk and C. Elliott. Finite elements on evolving surfaces. *IMA J. Numer. Anal.*, 27:262–292, 2007.

[7] G. Dziuk and C. Elliott. L^2-estimates for the evolving surface finite element method. *SIAM J. Numer. Anal.*, 2011. to appear.

[8] M. A. Olshanskii and A. Reusken. A finite element method for surface PDEs: matrix properties. *Numer. Math.*, 114:491–520, 2009.

[9] M. A. Olshanskii, A. Reusken, and J. Grande. An Eulerian finite element method for elliptic equations on moving surfaces. *SIAM J. Numer. Anal.*, 47:3339–3358, 2009.

[10] M. A. Olshanskii and V. Simoncini. Acquired clustering properties and solution of certain saddle point systems. *SIAM J. Matrix Anal. Appl.*, 31:2754–2768, 2010.

[11] J.-J. Xu and H.-K. Zhao. An Eulerian formulation for solving partial differerential equations along a moving interface. *J. Sci. Comput.*, 19:573–594, 2003.